Supplement of Atmos. Chem. Phys., 14, 6289–6299, 2014
http://www.atmos-chem-phys.net/14/6289/2014/
doi:10.5194/acp-14-6289-2014-supplement

Supplement of

Single particle diversity and mixing state measurements

R. M. Healy et al.

Correspondence to: R. M. Healy (robert.healy@utoronto.ca)

ATOFMS speciation estimates

In order to estimate the mass fraction of each chemical species in each single particle, ATOFMS measurements were constrained using concurrent HR-ToF-AMS and MAAP mass concentrations at hourly resolution. It is assumed that the summed relative peak area of marker ions associated with BC, OA, ammonium, nitrate and sulfate detected in the ATOFMS mass spectrum for a single particle are representative of the relative ratios of those species present in that single particle (Gross et al., 2000; Jeong et al., 2011). The following marker ions were chosen for OA: *m/z* 27 $[C_2H_3]^+$, 29 $[C_2H_5]^+$, 37 $[C_3H]^+$, 43 $[C_2H_3O]^+$, and BC: *m/z* 12, 24, 36, 48, 60, 72, 84 $[C_{1\text{-}7}]^+$ and *m/z* -12, -24, -36, -48, -60, -72, -84 $[C_{1\text{-}7}]^-$. The following ions were chosen to represent ammonium, sulfate, and nitrate: *m/z* 18 $[NH_4]^+$, -97 $[HSO_4]^-$, and -62 $[NO_3]^-$, respectively. The ions selected are consistent with previous studies (Spencer and Prather, 2006; Ferge et al., 2006; Jeong et al., 2011; Healy et al., 2013). Quantification of sodium and chloride was also explored, but the agreement observed with the concurrent measurements was poor. The average contribution of sodium and chloride to the measured $PM_{2.5}$ mass concentration was relatively low and therefore these species were omitted from the quantification procedure (Healy et al., 2013). Thus, for the mass reconstruction calculations, it is assumed that all particles are composed entirely of OA, BC, ammonium, sulphate and nitrate. These species have been demonstrated to account for more than 90% of annual average $PM_{2.5}$ mass concentrations in Paris (Bressi et al., 2013).

The ATOFMS relative peak area (RPA) for the marker ions in the number-weighted average mass spectrum collected for each hour of the campaign were compared directly to the average mass fractions of each chemical species present in the bulk aerosol for that same hour, as determined by concurrent HR-ToF-AMS/MAAP measurements. RPA was chosen for quantification because it is less sensitive to the variability in ion intensity associated with particle-laser interactions when compared to absolute peak area (Gross et al., 2000; Healy et al., 2013). RPA was calculated separately for positive ion and negative ion mass spectra. Comparison between the ATOFMS RPA values and the mass fraction data from the other instruments enabled the determination of arbitrary relative sensitivity factors (RSFs) for each species for each hour of the campaign. The ATOFMS is subject to different sensitivities for chemical species due to differences in their ionization energies, and matrix effects associated with different internal mixing states (Reilly et al., 2000; Reinard and Johnston, 2008; Pratt and Prather, 2009; Gross et al., 2000). The RSF values determined for each chemical species for each hour of the measurement period are shown in Fig. S1. It is important to note that relative sensitivity factors will vary depending upon the marker ions chosen to represent each species.

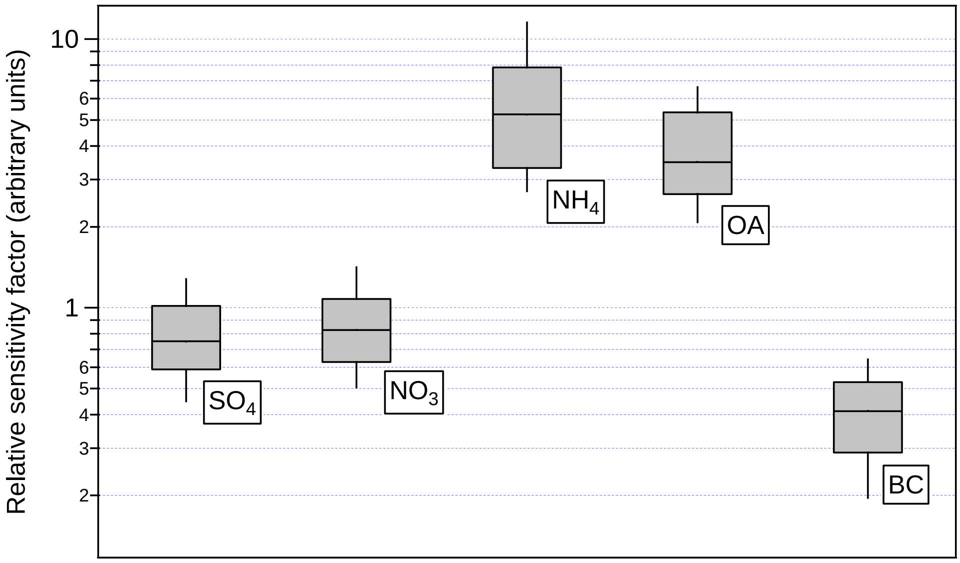

Fig. S1. Relative sensitivity factors derived every hour as the direct ratio of the relative peak area (summed for selected marker ions) in the average ATOFMS single particle mass spectrum for that hour with concurrent HR-ToF-AMS and MAAP measurements of the mass fraction of each species in the bulk aerosol (n = 610). Median, 75th percentile and 90th percentile are denoted by the solid line, box and whisker respectively.

The RSF values determined for each chemical species were observed to be relatively stable throughout the campaign. Changes in these values are expected to arise from changes in ATOFMS sensitivity to each chemical species depending on the particle matrix, or differing desorption/ionization efficiencies for different chemical mixing states (Gross et al., 2000; Wenzel et al., 2003; Kane and Johnston, 2000). Error will also be introduced by any size-dependence of desorption/ionization efficiency, instrument busy time and any potential effect of relative humidity upon mass spectral ion relative intensities (Neubauer et al., 1998; Kane and Johnston, 2000; Qin et al., 2006). The uncertainty (1σ) associated with hourly scaling factors derived for BC, OA, NH_4, SO_4 and NO_3 is 40%, 44%, 76%, 41% and 41%, respectively. The highest uncertainty is associated with ammonium, the species for which the ATOFMS also exhibits the poorest sensitivity. This uncertainty, however, is simply a measure of the suitability of the marker ion approach, and is not a direct measure of the uncertainty of speciation at the single particle level, which is not possible to confirm for field data.

Hourly RSF values are applied to each single particle mass spectrum to estimate the mass fractions of all five chemical species present in each single particle. The mass fraction of species i in particle j ($\mathrm{mf}_{i,j}$), is calculated as follows:

$$\mathrm{mf}_{i,j} = \frac{(\mathrm{RPA}_{i,j} \times \mathrm{RSF}_i)}{\sum_i(\mathrm{RPA}_{i,j} \times \mathrm{RSF}_i)}$$

Where $\mathrm{RPA}_{i,j}$ is the summed relative peak area of the marker ions for species i in particle j, and RSF is the relative sensitivity factor for species i for a particular hour of the campaign. Thus the sum of the mass fractions of all five species equal unity for each particle.

ATOFMS particle number concentrations in eight size bins were scaled at hourly resolution using simultaneous TDMPS data as described elsewhere (Healy et al., 2012). The uncertainty associated with the TDMPS is estimated to be <2% (Birmili et al., 1999). The total ATOFMS reconstructed mass concentration (assuming spherical shape and a particle density of 1.5 g cm^{-3}) in the size range 150-1067 nm is compared with the total HR-ToF-AMS/MAAP mass concentrations for BC, OA, NH_4, NO_3 and SO_4 in Figs. S2 and S3. Good agreement is observed, although the ATOFMS reconstructed mass is consistently lower. This is expected to be at least partly due to the fact that the ATOFMS does not detect particles smaller than 150 nm (d_{va}).

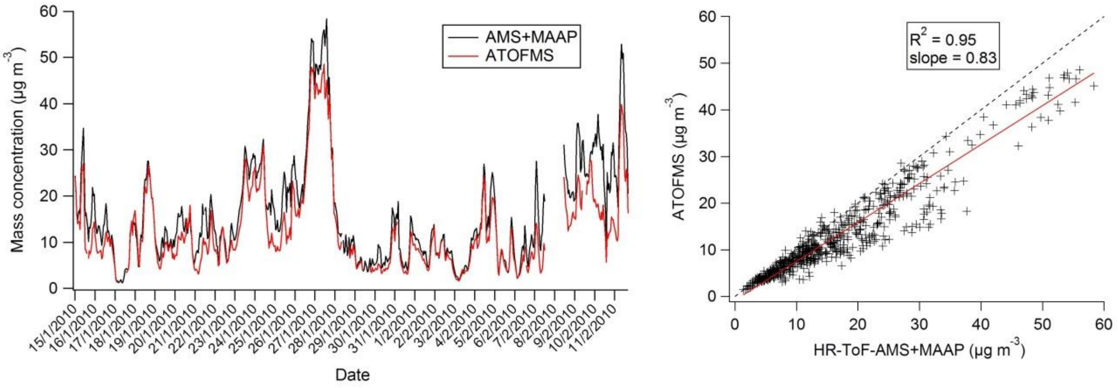

Fig. S2. Scaled ATOFMS mass concentration (150-1067 nm) and sum of total HR-ToF-AMS and MAAP mass concentrations for OA, BC, NH_4, NO_3 and SO_4. The dashed black line (right panel) represents the 1:1 fit. The red line (right panel) represents the orthogonal distance regression fit.

The estimated single particle mass fractions for each chemical species were summed across all particles and scaled to produce bulk aerosol mass concentration estimates. The ATOFMS-derived bulk aerosol mass fractions and the measured HR-ToF-AMS/MAAP bulk aerosol mass fractions for each hour of the measurement period are shown in Fig. S3. Good agreement is observed, although some discrepancy is apparent between the ATOFMS-derived bulk mass fractions and the HR-ToF-AMS/MAAP bulk mass fractions. This is expected to arise from the uncertainties associated with the ATOFMS measurements discussed earlier.

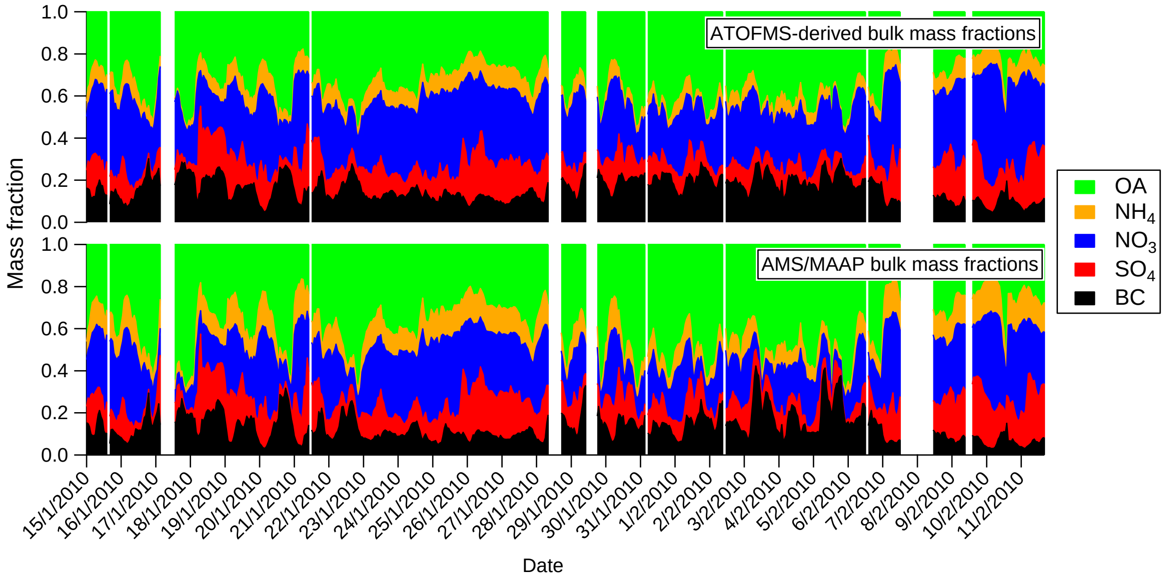

Fig. S3. Comparison of ATOFMS-derived bulk aerosol species mass fractions and HR-ToF-AMS/MAAP bulk aerosol species mass fractions.

When examining each species individually, good agreement is again observed between the ATOFMS-derived reconstructed mass concentrations and the HR-ToF-AMS/MAAP measured mass concentrations, as shown in Fig S4. Correlation coefficients (R^2) range from 0.84-0.93 and slopes range from 0.73 and 1.23. It is important to note that although the reconstructed mass concentrations track the measured mass concentrations well, there is no means by which to confirm whether the mass fraction species distributions at the single particle level are accurate. Thus, single particle speciation estimates should be interpreted with care, although those reported here are the best estimates available from the instrumentation deployed. A further improvement to the technique described here could involve the calculation of size-dependent scaling factors for each species using simultaneous

PTOF measurements of BC, OA, ammonium, nitrate and sulfate provided by a co-located soot particle aerosol mass spectrometer (Onasch et al., 2012). Size-resolved BC measurements were not available for the MEGAPOLI winter campaign.

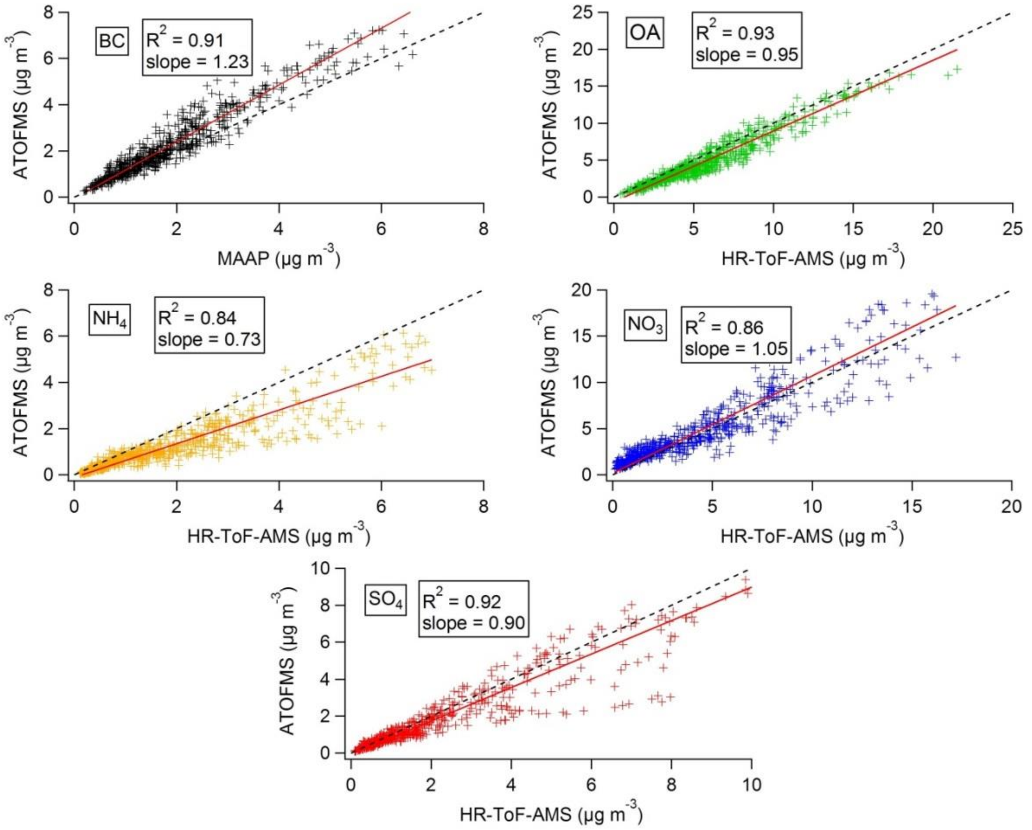

Fig. S4. Comparison of ATOFMS-derived and HR-ToF-AMS/MAAP measured mass concentrations for BC, OA, ammonium, nitrate and sulfate for each hour of the measurement period (n = 610). Black dashed lines represent the 1:1 fit, red lines represent the orthogonal distance regression fit. ATOFMS reconstructed mass concentrations have been multiplied by a factor of 1.2 (inverse of 0.83) to account for the underestimation of scaled ATOFMS mass concentrations relative to the total mass concentrations determined using the AMS/MAAP instruments (Fig. S2).

Dependence of ammonium nitrate mass concentrations upon temperature

As shown in Fig. S5, maximum diurnal ammonium and nitrate mass concentrations are observed when ambient temperatures are lowest between 02:00 and 10:00.

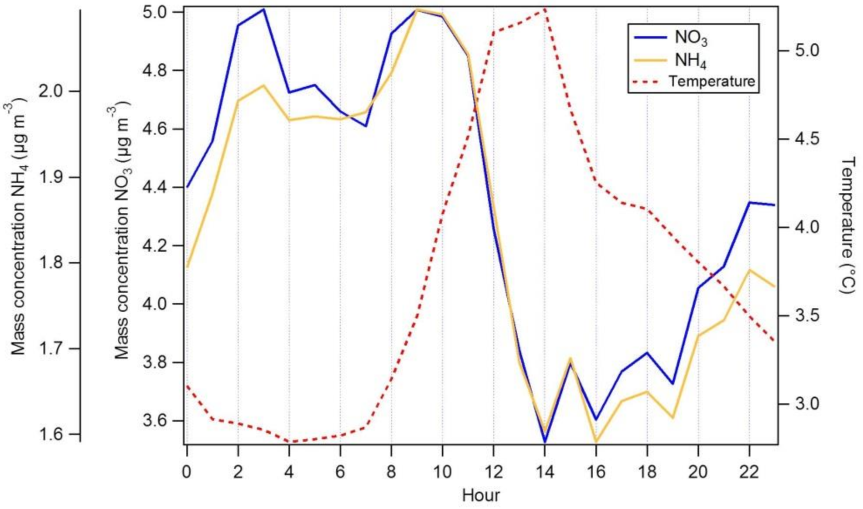

Fig. S5. Diurnal dependence of HR-ToF-AMS mass concentrations for nitrate and ammonium and ambient temperature.

References:

Birmili, W., Stratmann, F., and Wiedensohler, A.: Design of a DMA-based size spectrometer for a large particle size range and stable operation, Journal of Aerosol Science, 30, 549-553, Doi: 10.1016/s0021-8502(98)00047-0, 1999.

Bressi, M., Sciare, J., Ghersi, V., Bonnaire, N., Nicolas, J. B., Petit, J. E., Moukhtar, S., Rosso, A., Mihalopoulos, N., and Féron, A.: A one-year comprehensive chemical characterisation of fine aerosol (PM2.5) at urban, suburban and rural background sites in the region of Paris (France), Atmos. Chem. Phys., 13, 7825-7844, 10.5194/acp-13-7825-2013, 2013.

Ferge, T., Karg, E., Schröppel, A., Coffee, K. R., Tobias, H. J., Frank, M., Gard, E. E., and Zimmermann, R.: Fast Determination of the Relative Elemental and Organic Carbon Content of Aerosol Samples by On-Line Single-Particle Aerosol Time-of-Flight Mass Spectrometry, Environmental Science & Technology, 40, 3327-3335, 10.1021/es050799k, 2006.

Gross, D. S., Galli, M. E., Silva, P. J., and Prather, K. A.: Relative Sensitivity Factors for Alkali Metal and Ammonium Cations in Single-Particle Aerosol Time-of-Flight Mass Spectra, Analytical Chemistry, 72, 416-422, 2000.

Healy, R. M., Sciare, J., Poulain, L., Kamili, K., Merkel, M., Müller, T., Wiedensohler, A., Eckhardt, S., Stohl, A., Sarda-Estève, R., McGillicuddy, E., O'Connor, I. P., Sodeau, J. R., and Wenger, J. C.: Sources and mixing state of size-resolved elemental carbon particles in a European megacity: Paris, Atmos. Chem. Phys., 12, 1681-1700, 10.5194/acp-12-1681-2012, 2012.

Healy, R. M., Sciare, J., Poulain, L., Crippa, M., Wiedensohler, A., Prévôt, A. S. H., Baltensperger, U., Sarda-Estève, R., McGuire, M. L., Jeong, C. H., McGillicuddy, E., O'Connor, I. P., Sodeau, J. R., Evans, G. J., and Wenger, J. C.: Quantitative determination of carbonaceous particle mixing state in Paris using single-particle mass spectrometer and aerosol mass spectrometer measurements, Atmos. Chem. Phys., 13, 9479-9496, 10.5194/acp-13-9479-2013, 2013.

Jeong, C. H., McGuire, M. L., Godri, K. J., Slowik, J. G., Rehbein, P. J. G., and Evans, G. J.: Quantification of aerosol chemical composition using continuous single particle measurements, Atmos. Chem. Phys., 11, 7027-7044, 2011.

Kane, D. B., and Johnston, M. V.: Size and Composition Biases on the Detection of Individual Ultrafine Particles by Aerosol Mass Spectrometry, Environmental Science & Technology, 34, 4887-4893, 10.1021/es001323y, 2000.

Neubauer, K. R., Johnston, M. V., and Wexler, A. S.: Humidity effects on the mass spectra of single aerosol particles, Atmospheric Environment, 32, 2521-2529, http://dx.doi.org/10.1016/S1352-2310(98)00005-3, 1998.

Onasch, T. B., Trimborn, A., Fortner, E. C., Jayne, J. T., Kok, G. L., Williams, L. R., Davidovits, P., and Worsnop, D. R.: Soot Particle Aerosol Mass Spectrometer: Development, Validation, and Initial Application, Aerosol Science and Technology, 46, 804-817, 10.1080/02786826.2012.663948, 2012.

Pratt, K. A., and Prather, K. A.: Real-Time, Single-Particle Volatility, Size, and Chemical Composition Measurements of Aged Urban Aerosols, Environmental Science & Technology, 43, 8276-8282, 10.1021/es902002t, 2009.

Qin, X., Bhave, P. V., and Prather, K. A.: Comparison of Two Methods for Obtaining Quantitative Mass Concentrations from Aerosol Time-of-Flight Mass Spectrometry Measurements, Analytical Chemistry, 78, 6169-6178, 10.1021/ac060395q, 2006.

Reilly, P. T. A., Lazar, A. C., Gieray, R. A., Whitten, W. B., and Ramsey, J. M.: The Elucidation of Charge-Transfer-Induced Matrix Effects in Environmental Aerosols Via Real-Time Aerosol Mass Spectral Analysis of Individual Airborne Particles, Aerosol Science and Technology, 33, 135-152, 10.1080/027868200410895, 2000.

Reinard, M. S., and Johnston, M. V.: Ion Formation Mechanism in Laser Desorption Ionization of Individual Nanoparticles, Journal of the American Society for Mass Spectrometry, 19, 389-399, DOI: 10.1016/j.jasms.2007.11.017, 2008.

Spencer, M., and Prather, K.: Using ATOFMS to Determine OC/EC Mass Fractions in Particles, Aerosol Science & Technology, 40, 585-594, 10.1080/02786820600729138, 2006.

Wenzel, R. J., Liu, D.-Y., Edgerton, E. S., and Prather, K. A.: Aerosol time-of-flight mass spectrometry during the Atlanta Supersite Experiment: 2. Scaling procedures, J. Geophys. Res., 108, 8427, 10.1029/2001jd001563, 2003.